Influence of Nb Microaddition on Microstructure and Texture Evolution in a Fe-21Mn-1.3Al-1.5Si-0.5C TWIP Steel under Uniaxial Hot-Tensile Conditions

A.E. Salas-Reyes[1,2], I. Mejía[1] and J.M. Cabrera[3].

[1]*Instituto de Investigación en Metalurgia y Materiales, Universidad Michoacana de San Nicolás de Hidalgo, 58066-Morelia, Michoacán, México. E-mail: imejia@umich.mx, quique.salas@hotmail.com*

[2] *Departamento de Ingeniería Metalúrgica, Facultad de Química, Universidad Nacional Autónoma de México, Circuito Exterior s/n, Coyoacán, Cd. Universitaria, 04510-Ciudad de México, México.*

[3]*Departament de Ciència dels Materials i Enginyeria Metal·lúrgica, EEBE-Universitat Politècnica de Catalunya, c/Eduard Maristany 10-14, Edif. I, Of 1.18, 08019-Barcelona, Spain.*

ABSTRACT

Advanced high-strength steels as Twinning Induced Plasticity (TWIP) steels have been developed using microalloying elements and subsequent thermo-mechanical processing techniques. Moreover, under hot-working conditions, these steels undergo significant microstructural changes as a result of preferred crystallographic orientation (texture) of grains. In order to evaluate this behavior, one non-microalloyed and other single Nb-microalloyed TWIP steels were melted in an induction furnace and cast into metal and sand molds. Samples with austenitic grain sizes between 400 and 2000 μm were deformed at 800 °C and strained at a constant strain rate of 10^{-3} s^{-1}, and deformation state was examined by means of electron backscatter diffraction (EBSD) technique near to the fracture tip. It was found that non-microalloyed TWIP steel solidified in both metal and sand mold exhibits dynamically recrystallized grains. On the other hand, Nb microaddition has a strong influence in TWIP steel retarding the onset of recrystallization kinetics, showing low angle sub-structured grains. Furthermore, it was possible identifying the crystallographic orientation of grains using the inverse pole figures (IPF) and the orientation distribution function (ODF). Weak cube {001}<100> recrystallization and E{111}<110> γ-fiber deformation textures components were detected.

Key Words: steel, texture, stress/strain relationship.

INTRODUCTION

High-Mn austenitic steels with up to 30 wt.% Mn and more than 0.4 wt.% C have one of the best combination of the strength and plasticity among the currently available steels. This is due to the twinning-induced plasticity (TWIP) effect that occurs at room temperature but progressively transforms to dislocation glide when deformation temperature increases **[1]**. However, it has been shown that TWIP alloys have naturally low yield strength (YS) **[2]**. Accordingly, there is a clear benefit in increasing the yield strength through Nb, Ti, or V microalloying elements, operation that can be an ideal hardening mechanism to improve strength **[3]**. These microalloying elements can precipitate during the different stages of the steel production. During hot deformation, careful control of the processing parameters such as strain rate, temperature and strain is of great importance since they have significant influence on the deformation mechanisms, microstructural evolution and consequently mechanical properties of the deformed materials **[4]**. Thus, in order to achieve good final product properties, understanding texture formation during the hot rolling stage is an important topic.

In this way, a detailed knowledge of the austenite grain/subgrain structure and texture characteristics obtained during hot deformation is very important for the steel microstructure control during hot working. With Electron backscatter Diffraction (EBSD) individual grain orientations, local texture, and point-to-point orientation

relationships can be determined routinely on the surface of bulk samples **[5]**. Furthermore, understanding the microstructural distribution of strain in TWIP steels is fundamental to controlling the overall deformation at the macroscale. Particularly, most research work on texture development of TWIP steels has mainly focused on the behavior during cold rolling and annealing treatment. So, there is a lack of scientific information about their hot deformation behavior, which allows controlling microstructure and mechanical properties during hot rolling. Thus, the aim of this study is to determine the effect of single Nb-microaddition and solidification condition on the microstructure and texture evolution in TWIP steel under hot-tensile conditions.

EXPERIMENTAL PROCEDURE

The TWIP steel used in this study had the nominal chemical composition Fe-21wt.% Mn-1.3 wt.% Al-1.5wt.% Si-0.5wt.% C and 0.083wt.% Nb microaddition. Thus, two 70 mm x 60 mm cross section ingots were obtained from a 25 kg induction furnace, using high-pure raw materials for each composition. Additionally, these steel ingots were solidified into metal (MM) and sand molds (SM) and identified as non-microalloyed steel (TW-NM) and single Nb-microalloyed steel (TW-Nb). In order to be sure of the single austenite phase stabilization at room temperature, crystalline structure in the as-cast condition was determined in a Siemens D5000 X-ray diffractometer, using CuKα radiation and a 2θ diffraction angle ranging from 30° to 120°. On the other hand, hot tensile test were performed at 800 °C and strained at constant true strain rate of 10^{-3} s^{-1}, using cylindrical tensile specimens of 6 mm diameter and 30 mm gauge length. For this purpose, an Instron tensile machine equipped with a radiant cylindrical furnace was used.

First, the specimens were heated at 1100 °C and held for 900 s for microstructural homogenization purposes obtaining a similar austenite grain size. Then, the specimens were cooled down to the testing temperature (800 °C) at a cooling rate of 1.66 °C/s, and held again for 300 s. Finally, specimens were strained until failure and cooled down immediately after rupture into argon atmosphere in order to prevent samples oxidation. At this stage, the samples were cut along the loading direction close to fracture surface tip. EBSD specimens were mechanically ground, then prepolished using diamond pastes and finally carefully polished using colloidal silica solution. Every EBSD scan was carried out in the loading direction and the SEM magnification was 20x with a step size of 7 µm. The local austenite crystal lattice orientations and misorientations were determined using Kikuchi patterns produced in SEM by changing the direction of incident beam in a selected area channeling (SAC) **[6]**. Thus, the corresponding data acquisition and processing (crystallographic texture and deformation substructure) were carried out using the HKL Channel 5 software.

RESULTS AND DISCUSSION

Figure 1 (a-b) show typical X-ray diffraction patterns of the studied TWIP steels, in both solidification conditions, MM and SM. It can be seen that the chemical composition used in the fabrication of TWIP steels had allowed obtaining a stable austenitic (FCC) phase. However, it is also important to note that alloying elements affect many material properties such as lattice parameter, etc. Thus, during hot deformation of TWIP steel, the deformation mechanisms are strongly affected by the interaction of dislocations with crystal defects. In this way, the thermodynamic mechanism of dislocation movement is a thermally activated process **[7]** that greatly influences preferred orientations of crystals and microstructure **[8]**. Typical as-deformed microstructures of studied TWIP steels are shown in the EBSD quality maps in **Figure 2 (a-d)**. The dark lines represent high angle boundaries (>15°) and white lines indicate low angle boundaries (limited to misorientations angles from 2° to 15°), which refer to the substructure into the deformed grains. During hot deformation, dislocation density is high and therefore these dislocations are arranged in dislocation structures, which results in local misorientations of several degrees within the grains **[9]**. Moreover, it can be seen that TWIP steels solidified into metallic mold have a finer austenitic grain size than those solidified into sand mold. TW-NM/MM steel has approximately 400 µm grain size, while TW-Nb/SM steel has nearly 2000 µm in grain size.

In the case of TW-NM steel, some dynamic recrystallized grains are observed around high angle boundaries, with distinctive necklace structures; see **Figure 2 (a-b)**. This dynamically restoration mechanism plays an important role in controlling the microstructure and texture developed during hot working. Internal misorientations measurements allow separating dynamically recrystallized grains from deformed ones. If the internal grain misorientation is less than 1.55°, then grains are considered recrystallized grains, as indicate the blue color in the Kernel's maps that intentionally were superimposed in **Figure 2**. On the other hand, Nb-microaddition to TWIP steel has a strong effect in the substructure evolution during hot deformation. In this case, non-dynamically recrystallized grains were observed. So, a deformed condition is remaining after hot tensile tests, as

shown yellow and red colors in Kernel's maps in **Figure 2 (c-d)**. It has been revealed that Nb retards the onset of dynamic recrystallization by solute drag phenomenon and forming particles during hot deformation **[10]**.

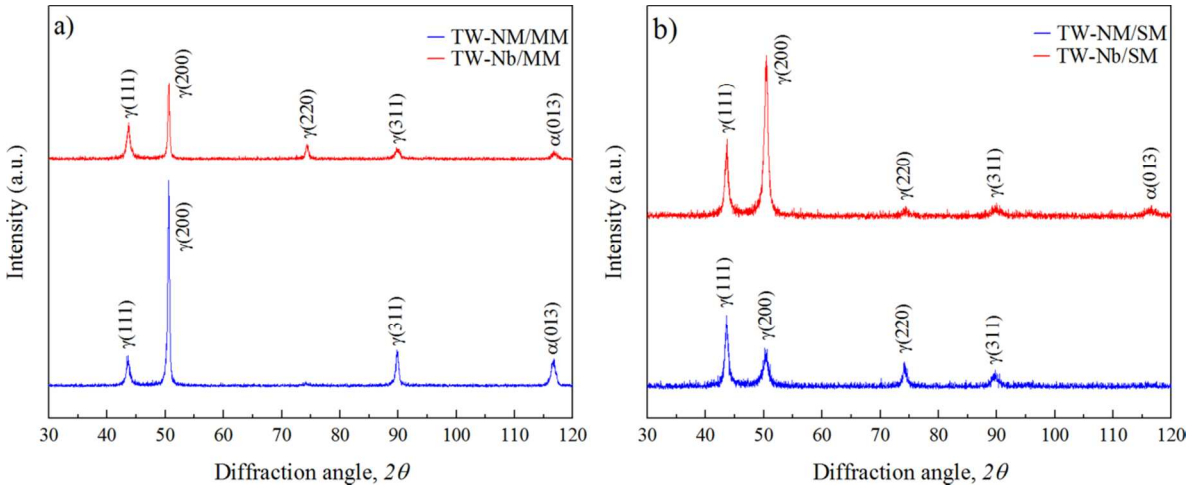

Figure 1. Typical X-ray diffraction patterns of studied TWIP steels: a) Metallic mold condition (MM) and b) Sand mold condition (SM).

Taking into account the above explanation for TW-NM and TW-Nb steels, **Figure 3 (a-d)** shows their pole figure and orientation distribution function (ODF) at $\phi 2=45°$ in the Euler space. In both solidification conditions, TW-NM steel displays intensity near to square corners. This behavior indicates a cube recrystallization component with grains oriented in the [012] preferred direction. It is worth noting that a very weak γ-fiber component is observed. Once recrystallization takes place, the deformation components are largely replaced by the recrystallization or cube components, being this behavior identified with the {001}<100> notation. In the case of TW-Nb steel, it is indicated the tendency to form the deformation γ-fiber texture due to low angle sub-structured grains, identified as E{111}<110> crystallographic components. In this case, it is important to note that niobium fine precipitates play an affective role in retarding austenite recrystallization due to pining force to inhibit grain boundary movement. So, accumulated strain and deformed structures are retained in austenite grains **[11]**. **Figure 4a** shows the inverse pole figure (IPF) map of TW-Nb/SM steel after hot-tensile test. It can be seen that a possible transition zone may be formed in the [101] crystallographic direction with a deformed condition from [122]/[233] to [215] crystallographic preferred orientations.

Additionally, the point-to-point misorientation of crystal lattices across high angle boundaries along the line A-B was measured, see **Figure 4b**. It is corroborated that sub-structured condition is present into grains, containing low angle boundaries with a misorientation values between 2 and 12 degrees along line A-B, as shown in **Figure 2 (c-d)**. It is also worth mentioning that high angle boundaries are indicated in the same line. These misorientation measurements help to explain why at current testing temperature relatively weak textures are formed under the applied strain rate.

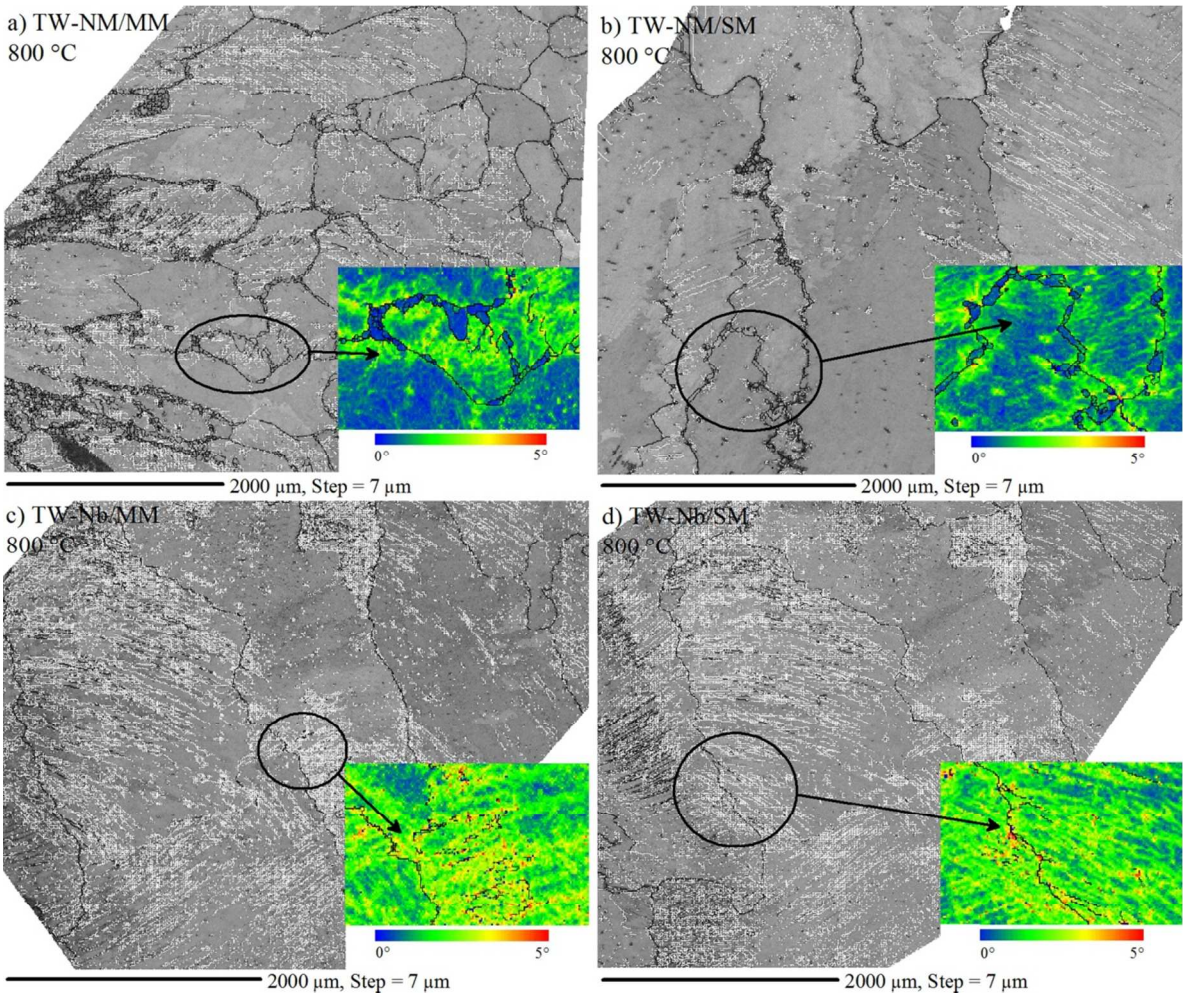

Figure 2. EBSD band contrast map for: a-b) Non-microalloyed TWIP steel solidified in MM and SM condition, and c-d) Nb-microalloyed TWIP steel solidified in MM and SM condition. Note that Kernel's maps were superimposed for each studied condition.

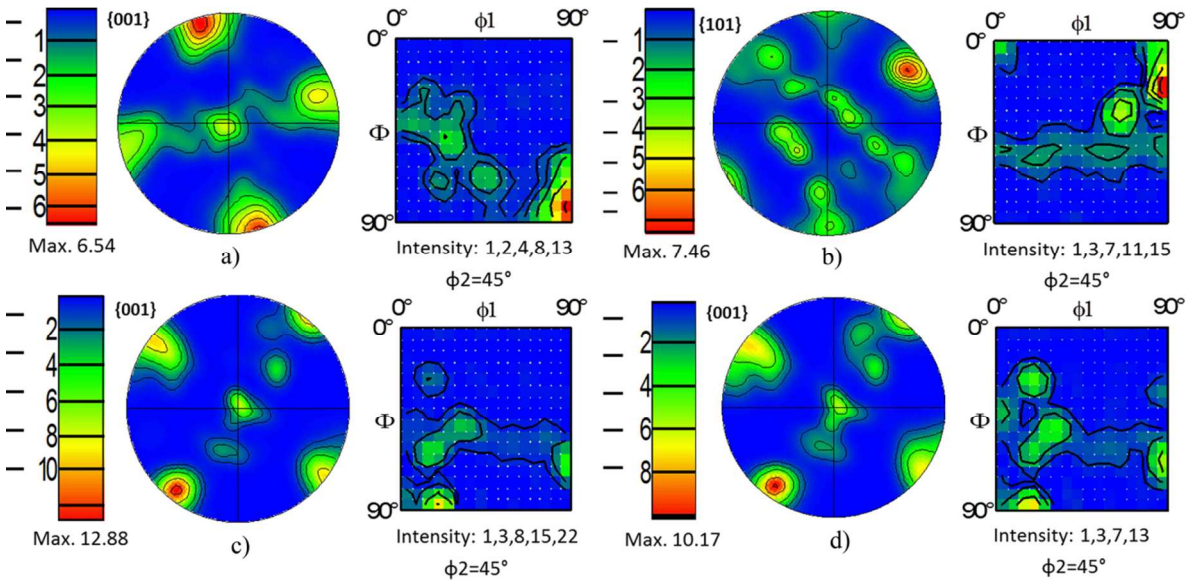

Figure 3. {001} Pole figures and orientation distribution function (ODF) at ϕ2=45° in the Euler space for studied TWIP steels in both solidification conditions: a) TW-NM/MM, b) TW-NM/SM, c) TW-Nb/MM and d) TW-Nb/SM.

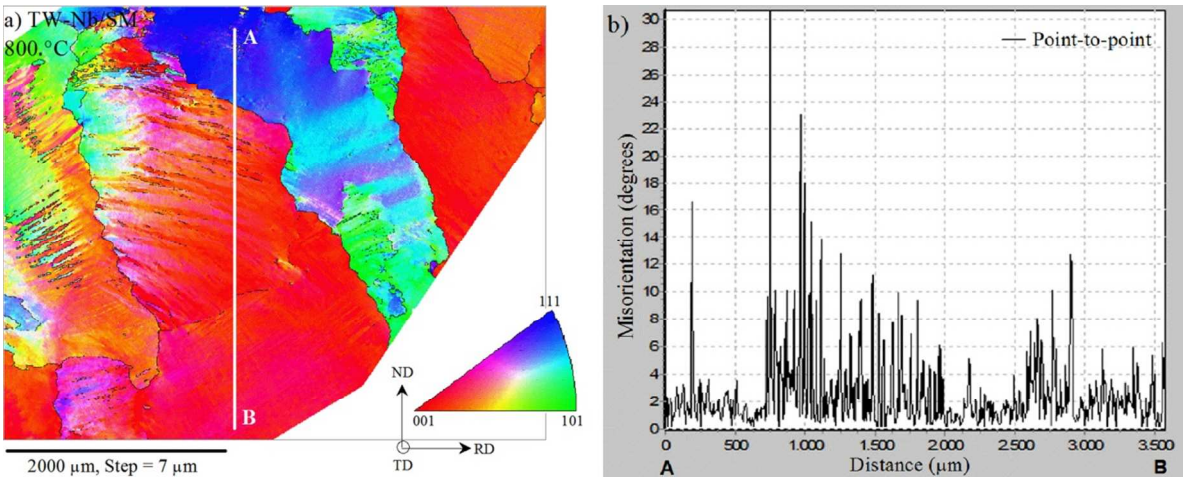

Figure 4. a) IPF map of Nb-microalloyed TWIP steel solidified in sand mold and b) Point-to-point misorientation measurement in line A-B.

CONCLUSIONS

The crystallographic and microstructure evolution of studied TWIP steels has been characterized by SEM-EBSD technique. The main conclusions are as follow:

1. For the chemical compositions and solidification conditions used in this study, the crystalline structure in the as-cast condition is composed of single austenite phase (FCC).
2. SEM-EBSD microstructure evolution indicates that these steels developed partial textures during hot deformation.
3. In general, weak Cube {001}<100> recrystallization and E{111}<110> γ-fiber deformation textures components were detected.

ACKNOWLEDGMENTS

Authors would like to thank the National Council on Science and Technology (Consejo Nacional de Ciencia y Tecnología-México) for the support during the project CB-2012-01-0177572. The present research project was also supported by the Coordinación de la Investigación Científica-UMSNH (México) (CIC-1.8). A.E. Salas-Reyes's studies were sponsored by the National Council on Science and Technology (Consejo Nacional de Ciencia y Tecnología-México), N.B. [242326].

References

1. E. Dryzek, M. Sarnek and M. Wróbel, *Nukleonika* **60**, 709 (2015).
2. O. Bouzaiz, S. Allain, C.P. Scott and P. Coggy, *Curr. Opin. Solid State Mater. Sci.* **15**, 141 (2011).
3. L. Llanos, B. Pereda and B. López, *Metall. Mater. Trans. A* **46**, 5248 (2015).
4. J. Zhang, H. Di, K. Mao, X. Wang, Z. Han and T. Ma, *Mater. Sci. Eng. A* **587**, 110 (2013).
5. Y.B. Zhang, A. Elbrond and F.X. Lin, *Mater. Charact.* **96**, 158 (2014).
6. Y. Randle, O. Engler, "The Kikuchi diffraction pattern", Chapter 6, *Introduction to texture analysis: macrotexture, microtexture and orientation mapping*, CRC Press, Taylor & Francis Group, 130 (2015).
7. H.J. McQueen, C.A.C. Imbert, *J. Alloys Comps.* **378**, 35 (2004).
8. D.S. Mcdarmaid, P.G. Partridge, *J. Mater. Sci.* **21**, 1525 (1986).
9. H. Mirzadeh, J.M. Cabrera, A. Najafizadeh, P.R. Calvillo, *Mater. Sci. Eng. A* **538**, 236 (2012).
10. A.J. DeArdo, *Inter. Mater. Rev.* **48**, 371 (2003).
11. I. Mejía, A.E. Salas-Reyes, A. Bedolla-Jacuinde, J. Calvo, J.M. Cabrera, *Mater. Sci. Eng. A* **616**, 229 (2014).